The Sensitive and Efficient Detection of Quadriceps Muscle Thickness Changes in Cross-Sectional Plane Using Ultrasonography: A Feasibility Investigation

Jizhou Li, Yongjin Zhou, *Member, IEEE*, Yi Lu, Guangquan Zhou, Lei Wang, *Member, IEEE*, and Yong-Ping Zheng, *Senior Member, IEEE*

***Abstract*—As a direct determinant parameter to quantify muscle activity, the muscle thickness (MT) has been investigated in many aspects and for various purposes. Ultrasonography (US) is a promising modality to detect muscle morphological changes during contractions since it is portable, noninvasive, and real time. However, there are few reports on sensitive and efficient estimation of changes of MT in a cross-sectional plane. In this feasibility investigation, we proposed a coarse-to-fine method based on a compressive-tracking algorithm for estimation of MT changes during an example task of isometric knee extension using ultrasound images. The sensitivity and efficiency are evaluated with 1920 US images from quadriceps muscle (QM) in eight subjects. The detection results were compared with those obtained from both traditional manual measurement and the well known normalized cross-correlation method, and the effect of the size of tracking window on detection performance was evaluated as well. It is demonstrated that the proposed method agrees well with the manual measurement. Meanwhile, it is not only sensitive to relatively small changes of MT but also computationally efficient.**

***Index Terms*—Compressive tracking, isometric knee extension, muscle thickness (MT), normalized cross correlation (NCC), quadriceps muscle (QM), sonomyography.**

Manuscript received March 20, 2013; revised June 24, 2013 and July 22, 2013; accepted July 23, 2013. Date of publication July 26, 2013; date of current version March 3, 2014. This work was supported in part by the Next Generation Communication Technology Major Project of National S&T under Grant 2013ZX03005013, in part by the Low Cost Healthcare Programs of the Chinese Academy of Sciences, in part by the Guangdong Innovative Research Team Program under Grant 2011S013, in part by International Science and Technology Cooperation Program of Guangdong Province under Grant 2012B050200004, and in part by the Hong Kong Innovation and Technology Commission under Grant GHP/047/09. (Corresponding author: Y. Zhou, phone: 086-134-2866-6265.)

J. Li, Y. Lu, and L. Wang are with the Shenzhen Institutes of Advanced Technology, Chinese Academy of Sciences, Shenzhen 518055, China.

Y. Zhou is with the Shenzhen Institutes of Advanced Technology, Chinese Academy of Sciences, Shenzhen 518055, China, and also with the Interdisciplinary Division of Biomedical Engineering, the Hong Kong Polytechnic University, Hung Hom, Hong Kong (e-mail: yj.zhou@siat.ac.cn).

G. Zhou and Y.-P. Zheng are with the Interdisciplinary Division of Biomedical Engineering, the Hong Kong Polytechnic University, Hung Hom, Hong Kong.

Color versions of one or more of the figures in this paper are available online at http://ieeexplore.ieee.org.

Digital Object Identifier 10.1109/JBHI.2013.2275002

I. Introduction

ULTRASONOGRAPHY (US) is widely used in the field of measuring morphology changes of skeletal muscles due to its advantages, such as being stable, easy to use, low cost, and able to record instantaneous activities from deeper muscles without crosstalk from adjacent ones [1]. In recent years, US has been proved to be able to accurately measure the changes in muscle thickness (MT) [1]–[6], pennation angle or fiber orientation [7]–[12], fiber length [6]–[8], [13]–[15], fascicle curvature [16], [17], and cross-sectional area [18]–[20] during contractions. Because these architectural parameters could change significantly during contraction, they potentially provided a valid method of characterizing activities of various muscles. Zheng *et al.* [21] used sonomyography to describe the real-time architectural parameters' change detected using B-mode ultrasound images during the muscle contraction and proposed to use it for the prosthetic control [21]–[23], assessment of isometric muscle contraction, [2], [10], [20], [24] and isotonic contraction [25].

Among these morphological parameters, MT has the potential to be the most direct determinant to quantify muscle activity in a cross-sectional plane. Previous studies have shown that changes in MT, measured with ultrasound, are a valid index to provide insight into muscle contraction as compared with electromyography (EMG) [26]. Miyatani *et al.* [27] used the MT to estimate the muscle volume of the quadriceps femoris based on US; Raney *et al.* [28] used the MT to document the effects of the spinal manipulation on muscle contraction behavior, and Ohata *et al.* [29] employed MT to quantify the muscle strength of people with severe cerebral palsy. English *et al.* [30] validated that ultrasound was a reliable measure of the MT in acute-stroke patients for some anatomical sites. However, MT was traditionally measured by an experienced operator, and the process is not only subjective, but also time-consuming. Recently, researchers have presented several computer-aided methods which could be used to estimate the MT or related parameters. In longitudinal direction, we previously proposed an automatic tracking strategy to achieve the continuous and quantitative measurement for MT of gastrocnemius muscle in ultrasound images [5]. Darby *et al.* [31] proposed a method to automatically track movement of features, in localized tissue portions. And they provided an automated approach, which has no strong assumptions on the

fascicle shape, to estimate the skeletal muscle fascicle curvature [16]. Loram *et al.* [13] used an interpolated control-points-based normalized cross-correlation (NCC) method to track continuous changes in a human muscle contractile length in a longitudinal direction, where the ultrasound echo of the muscle would exhibit certain spatial consistency in adjacent regions. In a cross-sectional plane, Shi *et al.* [2] demonstrated the feasibility of using the changes of MT extracted from the NCC method to characterize the muscle fatigue. Two rectangular windows were selected for the upper and lower boundaries of the biceps brachii in the cross-sectional plane, and a cross-correlation algorithm was used to measure the distance between their centers as MT at each moment. Koo *et al.* [32] used an automated muscle-boundary-tracking algorithm based on the NCC method to track the pectoralis major muscle boundaries during dynamic contraction. The detections of the muscle motion and patterns in a cross-sectional plane have also been employed to investigate the finger flexion motion and finger positions [33], [34].

However, for a sensitive and efficient detection of MT changes in the cross-sectional plane, the NCC method has several drawbacks. Apart from an intensive calculation requirement, a more general problem with NCC is the choice of the tracking window size [13]. The larger the window size is, the more robust while less sensitive to fine changes of MT, the tracking would be, and *vice versa*. We believe that both sensitivity and efficiency to fine changes detection of MT are crucial in muscle study based on ultrasound image sequences, which are commonly acquired nowadays at frame-rate of 12–30 Hz and the interframe muscle motion is usually relatively small. Therefore, in this study, an effective coarse-to-fine method, based on the compressive-tracking algorithm [35] followed by a fine-tuning step, is proposed to detect thickness changes in quadriceps muscle (QM) in a cross-sectional plane.

II. Methods

A. Subjects and Experiment Protocol

Eight healthy subjects (six male and two female, mean $\pm$ SD, age $= 33.6 \pm 5.2$ years; body weight 65.9 ± 11.7 kg; height $= 165 \pm 7.0$ cm) volunteered to participate in this study. No participant had a history of neuromuscular disorders, and all were aware of experimental purposes and procedures. Human subject ethical approval was obtained from the relevant committee in the Hong Kong Polytechnic University, Hung Hom, Hong Kong, and an informed consent was obtained from the subject prior to the experiment. The testing position of the subject was in accordance with the User's Guide of a Norm dynamometer (Humac/Norm Testing and Rehabilitation System, Computer Sports Medicine, Inc., MA, USA). Each subject was seated with both the right hip and knee at angles of 90° and was required to put forth his/her maximal effort of isometric knee extension for a period of 3 s, with verbal encouragement provided. The maximal voluntary contraction (MVC) was defined as the highest value of the torque recorded during the entire isometric knee extension. The MVC torque was then calculated by averaging the two recorded highest torque values from the two tests under the same conditions. The subject performed several warm-up trials to get familiar with the experiment protocol. After a rest of 5 min, the subject was instructed to perform ramp increasing then decreasing contractions, up to 90% of his/her MVC, using isometric knee extension. During each contraction, a torque production template, serving as a target, and the subject's real-time torque signal were displayed together on a computer screen placed in front of him/her. Each test was repeated twice with a rest of 5 min between two adjacent trials. The torque was measured by the aforementioned dynamometer and the reason for choosing 90% MVC as the highest value was to avoid muscle fatigue.

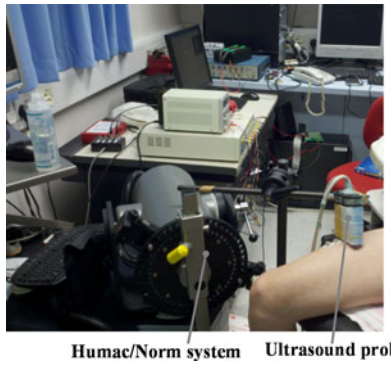

Fig. 1. Experimental setup for collecting ultrasound images from the subject's right QM during isometric knee extension. The ultrasound probe was aligned perpendicularly to QM belly using a multidegree adjustable bracket.

B. Data Acquisition and Data Processing

A real-time B-mode ultrasonic scanner (EUB-8500, Hitachi Medical Corporation, Tokyo, Japan) with a 10 MHz electronic linear array probe (L53L, Hitachi Medical Corporation, Tokyo, Japan) was used to obtain ultrasound images of muscles. The long axis of the ultrasound probe was arranged perpendicularly to the long axis of the thigh on its superior aspect, 40% distally from the knee (measured from the anterior superior iliac spine to the superior patellar border) [36], [37]. The ultrasound probe was fixed by a custom-designed foam container with fixing straps, and a very generous amount of ultrasound gel was applied to secure the acoustic coupling between the probe and skin during muscle contractions, as shown in Fig. 1. The probe was adjusted to optimize the contrast of muscle fascicles in ultrasound images [1], and the position was marked to ensure that the probe was placed at the same site every time. Then, the B-mode ultrasound images were digitized by a video card (NI PCI-1411, National Instruments, Austin,TX, USA) at a rate of 25 frame/s for later analysis. Before the test began, an ultrasound image was collected from the subject on the RF muscle under the relaxed condition as a reference. A total of 8 (subjects) $\times$ 240 (frames) ultrasound images with 556 $\times$ 418 pixels were acquired, and all the images were cropped to keep the image content only. Ultrasound images and torque signals were simultaneously collected and stored by custom-developed software for the ultrasonic measurement of motion and elasticity (UMME, http://www.tups.org) for further analysis. The time delay between the different data collection systems was calibrated using

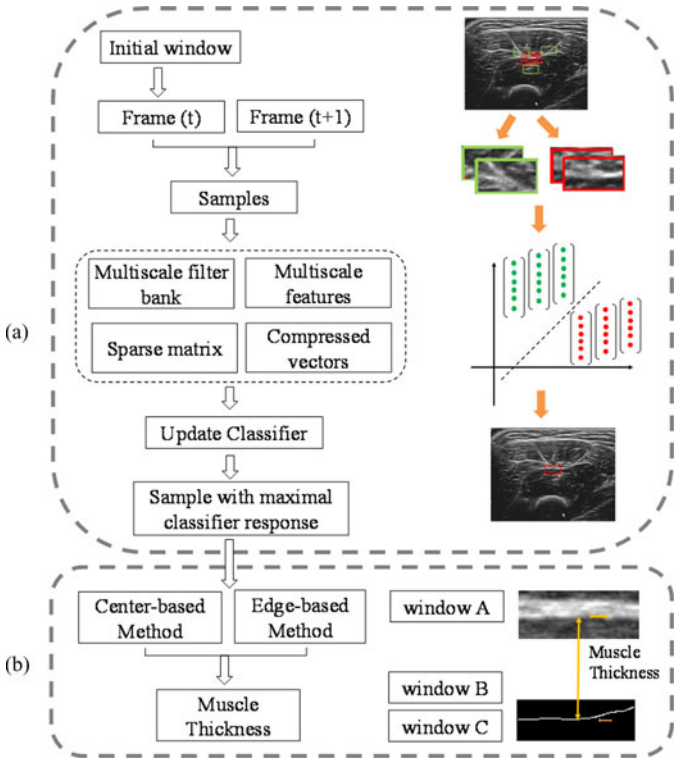

Fig. 2. Diagrammatic illustrations of the proposed method. (a) Coarse position-locating of the tracked window using a compressive-tracking algorithm, and (b) Finetuning to estimate the MT using the center-based method and edge-based method.

a method similar to that described by our earlier study [38]. A given B-mode ultrasound image frame corresponded to a given torque value point.

All signals were processed offline, using programs written in MATLAB (Version 7.12, MathWorks, Inc., Natick, MA, USA) on a PC equipped with Windows 7, Intel (R) Core i3 3.30 GHz processors and 2 GB RAM.

C. Coarse Locating

The proposed coarse-to-fine method for the automatic detection of MT changes includes two stages: coarse locating and fine-tuning, as shown in Fig. 2. The first stage of our method is to extract coarse location using the compressive-tracking algorithm [35]. Here, the tracking problem is formulated as a detection task. In the first frame of each ultrasound image sequence, three initial tracking windows are selected manually along the top and bottom of the RF muscle and femur, respectively. In this selection procedure, each window is placed such that its horizontal center line lies at the exact boundary of RF muscle or femur, as shown in Fig. 3. The sizes of these windows are chosen empirically to include sufficient features for a reliable tracking. At each incoming frame, some positive samples (near the current target location) and negative samples (far away from the object center) will be sampled to update the classifier. To predict the object location in the next frame, some samples around the current target location are drawn and the one with the maximal classification score is treated as the expected location. The main steps of compressive tracking are briefed in the Appendix A.

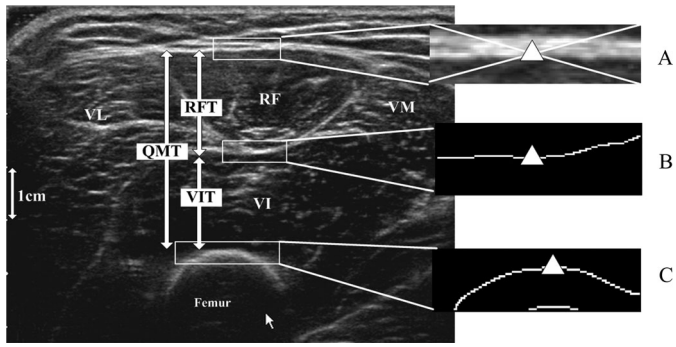

Fig. 3. Illustration of MT definitions. Three initial tracking windows A, B, and C are selected to obtain RFT, VIT, and QMT. B and C have been handled by the Canny edge detector and the maximal connected components search technology. The triangles point out the locations of the selected window A, window B, and window C, respectively.

D. Fine-Tuning Step

The MT at each moment is defined as the vertical distance among windows location. Specifically speaking, the thickness of rectus femoris muscle (RFT) is defined as the maximum vertical distance between window A and window B, the thickness of vastus intermedius muscle (VIT) is defined as the maximum vertical distance between window B and window C, and the thickness of QM is defined as the minimum vertical distance between window A and window C. The locations of these windows will be determined by two different ways, which will be stated as follows and illustrated in Fig. 3:

1) *Edge-based method:* The compressive-tracking algorithm provides a rough location of the tracked window. Then, for windows B and C, the Canny edge detector and maximal connected components search will be used to extract the edge. The Canny edge detector transfers the window image to a binary image, and then maximal connected components search technology will be used to find the exact boundary of interests, as illustrated in Fig. 3.
2) *Center-based method:* There exist multiple boundaries for window A, after applying the canny edge detector. Therefore, the location of window A will be calculated as the center of this corresponding window, as illustrated in Fig. 3.

E. Methods Evaluation

The manually derived measurement by the investigator using ImageJ software (ImageJ, National Institutes of Health, USA) was treated as the golden standard (true MT), and the true thickness was calculated as the average manually measured vertical distance of two boundaries by two investigators. This manual measurement was repeated three times by each investigator. It has a high degree of repeatability ($R^2 = 0.984, P < 0.001$) and reproducibility ($R^2 = 0.961, P = 0.003$). A quantitative assessment of the detection accuracy was obtained by evaluating the percentage change rate (PCR) of the muscle defined

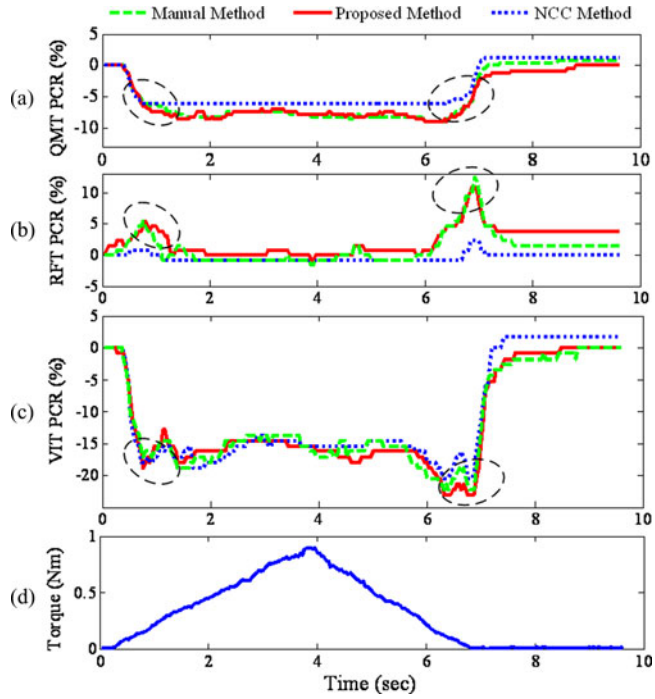

Fig. 4. Comparison of PCRs for RFT, VIT, and QMT. (a) PCRs of QMT by the manual, proposed, and NCC methods, respectively, on the data from a representative subject. (b) PCRs of RFT bythe manual, proposed, and NCC methods, respectively. (c) PCRs of VIT by manual, proposed, and NCC methods, respectively. (d) Torque signal during the corresponding isometric knee extension.

as follows:

$$\text{PCR}(\%) = \frac{T - T_0}{T_0} \times 100\%$$

where T was the resultant MT at each frame, and T_0 was the reference MT, which was captured under the relaxed condition. The NCC method, see Appendix B for details, was implemented to detect the MT change and the same window size was selected. Bias and jitter are used as metrics to quantify the performance of the method. Bias is the mean of the difference error of PCR, which is compared with the manually derived measurement, and jitter represents the error of the bias, i.e., jitter is measured as the standard deviation of the displacement error [39].

III. Results

A. Detection of MT Changes

Fig. 4(a)– (c) showed a typical PCR result of QMT and RFT from a representative subject. The synchronized torque signal at the same time was shown in Fig. 4(d). In this example, there was an obvious thickness increase of RF muscle when the muscle began to contract and when the muscle almost finished relaxing, as labeled by ellipses with dotted lines. The two methods, both, detected these changes successfully. However, the proposed method demonstrated more sensitivity to fine changes of MT with more amplitude details during the muscle struggling to reach its MVC and beginning to relax than the NCC method. Fig. 5 showed the jitter and bias for difference errors of PCR from all subjects.

B. Computational Time

The size of windows A, B, and C were selected as 100×40, 160 × 40, and 100 ×40, respectively. The interframe computation cost of window B, as an example, was shown in Table I. It is found in this example that NCC method required significantly more time than the proposed method. It should be noted that, the computational cost is dependent on the window size, which will be investigated in the following section.

C. Effect of the Window Size

To look into the effect of different choices of the tracking window size, taking window B of subject #1 as an example, the tracking window was placed such that its horizontal center line lies at the bottom boundary of RF muscle and the window size was then varied in terms of both the width and height. Specifically speaking, the width varied from 30 to 300 pixels with a step of $ws = 10$ and the height varied from 20 to 200 pixels with a step of $hs = 10$. In other words, the tracking of window B for 239 incoming frames of subject #1 was run for a total of 28 times, and the results is shown in Fig. 6(a), where the color from blue to red indicates the increasing of mean difference of all frames between the proposed method and the manual measurement. The result of the same experiment but using the NCC method is shown in Fig. 6(b). The computation costs corresponding to Fig. 6(a) and (b) are illustrated in Fig. 6(c), where the color from blue to red indicates the increasing of computation cost.

IV. Discussion

The main objective of this preliminary investigation is to provide a sensitive and efficient solution for the detection of QM thickness changes in the cross-sectional plane. The first merit of the proposed method is the reduced computation cost compared to NCC method, which has been employed for MT measurement previously [2], [32]. On the data from eight normal subjects it is found that for the fine-tuning step, the center-based method required about 1.5×10^{-5} s and the edge-based method required less than 6 ms, when the window sizes were 100 (window A) and 120 × 40 (window B), respectively. Taking the slightly more time-consuming window B for example, as shown in Table I, the proposed method, including coarse locating and fine-tuning, used less than 60 ms, while the NCC method needed nearly 190 ms on the MATLAB platform. It is expected to run even faster in a C/C++ implementation and be potentially available for an online and frame-by-frame estimation of MT.

It is also very interesting to find RF and VI thickness change dramatically, at the beginning of the ramp increasing and end of ramp decreasing, as labeled by ellipses with dotted lines in Fig. 4. Meanwhile, in the span between the two ellipses, the proposed method produced more sensitive thickness estimation than the NCC method, as shown in Fig. 4, where most of the time NCC results remained constant. The examination of an individual muscle, such as RF and VI, can provide a partial snapshot of the quadriceps activity.

The study aimed at the automatic measurement of MT in a cross-sectional plane, which is now realized with sensitivity

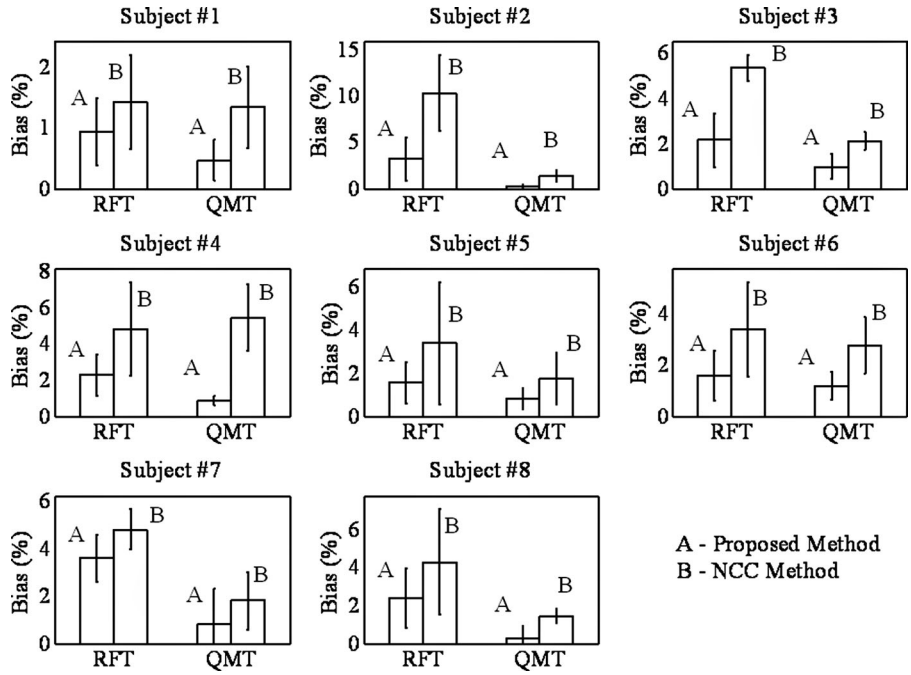

Fig. 5. Bias and jitter in terms of PCR (to manual method) for RFT and QMT.

TABLE I
COMPARISON OF INTERFRAME COMPUTATIONAL TIME (MEAN ± STANDARD DEVIATION)

	Inter-frame computational time (ms)	
Subject	Proposed Method	NCC Method
1	59.31 ± 3.15	177.56 ± 3.48
2	46.76 ± 4.02	180.17 ± 2.90
3	51.49 ± 2.76	153.23 ± 7.59
4	57.43 ± 5.46	187.46 ± 9.29
5	55.13 ± 2.58	165.15 ± 2.51
6	64.20 ± 1.43	182.78 ± 4.21
7	63.01 ± 8.86	182.55 ± 2.15
8	79.34 ± 1.78	165.46 ± 2.97

and efficiency. Meanwhile, we would like to point out that one example of the new findings made possible the fine details revealed in Fig. 4, where the VIT and RFT change nonlinearly, while the torque output remain roughly linear during an isometric knee extension, and interestingly, the inverse patterns of the MT change in VI and RF echo to the EMG findings by Akima *et al.* [40]. It should be noted that, for RF, the proposed implementation made such fine observations possible while the popular NCC almost flatten the changes out. Yet, data from more subjects than current are needed to confirm or explain the extraordinary nonlinear RFT and VIT patterns.

In terms of bias and jitter, as shown in Fig. 5, the proposed method also outperformed the NCC method. It should also be noted that the size of the tracking window is an important parameter for both the NCC method and proposed method. As we know, the NCC method is sensitive to the size of tracking window [13]. The larger the window size (to be more concise,

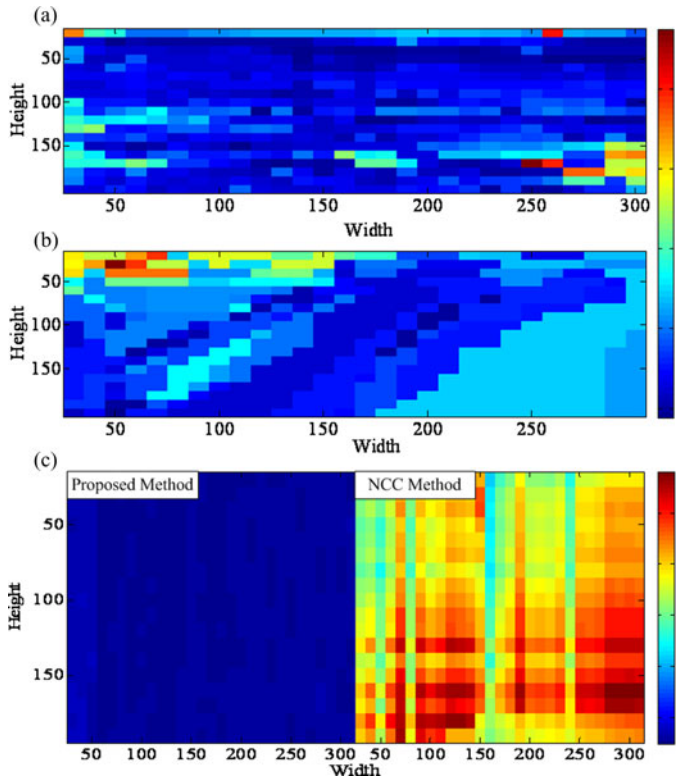

Fig. 6. Effects of the window size on the performance of tracking methods. (a) Mean difference of all frames between tracking results from proposed method and manual measurement. Color variation from blue to red indicates difference levels from low to high. (b) Mean difference of all frames between tracking results from the NCC method and manual measurement. (c) Computation cost comparison between the proposed and NCC method, where the color variation from blue to red indicates the computation cost from low to high.

for windows A, B, and C, which are more longitudinally oriented than vertically oriented, the width of the window size) is, the more robust while less sensitive the tracking would be, and *vice versa*. As shown in Fig. 6, the effect of the window size variation on the detection performance of the proposed method and NCC method exhibited different patterns, but both methods have certain choices of window size where the tracking performance is relatively satisfactory in terms of the measurement difference as compared to results from the manual method. This study is currently focused mainly on the feasibility of sensitive and efficient detection of the MT changes in a cross-sectional plane under a convenient experiment setup. To promote the proposed method for clinical application in pattern extraction of changes in MT, it would be necessary to increase the number of subjects and involve a greater range of tasks to comprehensively evaluate and accordingly improve the proposed method in future.

V. Conclusion

The results presented in this feasibility investigation provide insight into the algorithmic and computational considerations required to implement sensitive and efficient detection of MT changes in a cross-sectional plane. The computation cost, sensitivity, and effect of the size of tracking window were investigated, and the results were compared with those obtained from both traditional manual measurement and well-known NCC method. On 1920 US images from QM in eight subjects, it is demonstrated that the proposed method agrees well with the manual measurement and can outperform the cross-correlation method in terms of computation cost and sensitivity to fine changes of MT.

Appendix

A. Compressive Tracking Algorithm

The main steps of the compressive-tracking algorithm [35] are summarized as follows. The parameters such as α and β are decided empirically based on numerous tests.

Input: tth image frame.

1) Sample a set of image patches, $D^{\gamma} = \{\mathbf{z} | \|\mathbf{l}(\mathbf{z}) - \mathbf{l}_{t-1}\| < \gamma\}$ where l_{t-1} is the tracking location at the (t-1)th frame, and extract the features with nonadaptive low dimensionality based on compressive sensing theories.
2) For each sample $\mathbf{z} \in \mathbb{R}^m$, its low-dimensional representation is $\mathbf{v} = (v_1, \ldots, v_n)^{\mathbb{T}} \in \mathbb{R}^n$ with $m \gg n$. All elements in $\mathbf{v}$ are assumed to be independently distributed. A naive Bayes classifier H is used to feature each vector,

$$H(\mathbf{v}) = \log\left(\frac{\prod_{i=1}^{n} p(v_i|y=1)p(y=1)}{\prod_{i=1}^{n} p(v_i|y=0)p(y=0)}\right) = \sum_{i=1}^{n} \log\left(\frac{v_i|y=1}{v_i|y=0}\right) \quad (1)$$

where $p(y=1) = p(y=0)$, $y \in \{0,1\}$ is a binary variable which represents the sample label. The conditional distributions $p(v_i|y=1)$ and $p(v_i|y=0)$ in the classifier $H(\mathbf{v})$ are assumed to be Gaussian distributed with four parameters $(\mu_i^1, \sigma_i^1, \mu_i^0, \sigma_i^0)$, where

$$p(v_i|y=0) \sim N(\mu_i^0, \sigma_i^0), p(v_i|y=1) \sim N(\mu_i^1, \sigma_i^1) \quad (2)$$

and the maximal classifier response is used to find the tracking location $\mathbf{l}_t$.

3) Sample two sets of image patches, $D^{\alpha} = \{\mathbf{z} | \|\mathbf{l}(\mathbf{z}) - \mathbf{l}_t\| < \alpha\}$ and $D^{\zeta,\beta} = \{\mathbf{z} | \zeta < \|\mathbf{l}(\mathbf{z}) - \mathbf{l}_t\| < \beta\}$ with $\alpha < \zeta < \beta$.
4) Extract the Haar-like features with these two sets of samples and the scalar parameters in (2) are incrementally updated by

$$\begin{cases} \mu_i^1 \leftarrow \lambda\mu_i^1 + (1-\lambda)\mu^1 \\ \sigma_i^1 \leftarrow \sqrt{\lambda(\sigma_i^1)^2 + (1-\lambda)(\sigma^1)^2 + \lambda(1-\lambda)(\mu_i^1 - \mu^1)^2} \end{cases} \quad (3)$$

Output: Tracking location $\mathbf{l}_t$ and classifier parameters.

B. Normalized 2-D Cross Correlation

The NCC algorithm is to determine the location of a desired pattern represented by a template function t inside a 2-D image function f. The template is shifted pixel-by-pixel across the image, forming a correlation plane that provides information of where the template best matches the image. Let $f(x,y)$ be the intensity value of the $M \times N$ image f at pixel $(x,y), x \in 0, \ldots, M-1, y \in 0, \ldots, N-1$ and let $t(x,y)$ be the intensity value of the $m \times n$ at pixel (x,y) where $m < M, n < N$. All the NCC coefficients are stored in a correlation matrix $\gamma_{u,v}$ defined:

$$\gamma_{u,v} = \frac{\Sigma_{x,y}(f(x,y) - \overline{f}_{u,v})(t(x-u, y-v) - \overline{t})}{\sqrt{\Sigma_{x,y}(f(x,y) - \overline{f}_{u,v})^2 \Sigma_{x,y}(t(x-u, y-v) - \overline{(t)})^2}} \quad (4)$$

where $u \in 0, 1, \ldots, M-N, v \in 0, 1, \ldots, m-n$, $\overline{f}_{u,v}$ denotes the mean value of $f(x,y)$ within the area of the template t shifted by (u,v) steps and defined:

$$\overline{f}_{u,v} = \frac{1}{N \times n} \sum_{x=u}^{u+N-1} \sum_{y=v}^{v+n-1} f(x,y) \quad (5)$$

and $\overline{t}$ denotes the mean value of the template t defined in a similar way.

References

[1] P. Hodges, L. Pengel, R. Herbert, and S. Gandevia, "Measurement of muscle contraction with ultrasound imaging," *Muscle Nerve*, vol. 27, no. 6, pp. 682–692, 2003.
[2] J. Shi, Y.-P. Zheng, X. Chen, and Q. Huang, "Assessment of muscle fatigue using sonomyography: Muscle thickness change detected from ultrasound images," *Med. Eng. Phys.*, vol. 29, no. 4, pp. 472–479, 2007.
[3] K. Thoirs and C. English, "Ultrasound measures of muscle thickness: Intra-examiner reliability and influence of body position," *Clin. Physiol. Funct. Imag.*, vol. 29, no. 6, pp. 440–446, 2009.
[4] P. Han, Y. Chen, L. Ao, G. Xie, H. Li, L. Wang, and Y. Zhou, "Automatic thickness estimation for skeletal muscle in ultrasonography: Evaluation of two enhancement methods," *BioMed. Eng. OnLine*, vol. 12, no. 6, 2013.
[5] S. Ling, Y. Zhou, Y. Chen, Y.-Q. Zhao, L. Wang, and Y.-P. Zheng, "Automatic tracking of aponeuroses and estimation of muscle thickness in

ultrasonography: A feasibility study," *IEEE J. Biomed. Health Informat.*, to be published. DOI: 10.1109/JBHI.2013.2253787.
[6] A. Randhawa and J. M. Wakeling, "Associations between muscle structure and contractile performance in seniors," *Clin. Biomech.*, vol. 28, no. 13, pp. 705–711, Jun. 17, 2013.
[7] G. Chleboun, A. France, M. Crill, H. Braddock, and J. Howell, "*In vivo* measurement of fascicle length and pennation angle of the human biceps femoris muscle," *Cells Tissues Organs*, vol. 169, no. 4, pp. 401–409, 2001.
[8] C. Maganaris, V. Baltzopoulos, and A. Sargeant, "Repeated contractions alter the geometry of human skeletal muscle," *J. Appl. Physiol.*, vol. 93, no. 6, pp. 2089–2094, 2002.
[9] Y. Zhou, J. Z. Li, G. Zhou, and Y.-P. Zheng, "Dynamic measurement of pennation angle of gastrocnemius muscles during contractions based on ultrasound imaging," *BioMed. Eng. OnLine*, vol. 11, no. 63, 2012.
[10] Y. Zhou and Y.-P. Zheng, "Estimation of muscle fiber orientation in ultrasound images using revoting Hough transform (RVHT)," *Ultrasound Med. Biol.*, vol. 34, no. 9, pp. 1474–1481, 2008.
[11] Y. Zhou and Y.-P. Zheng, "Longitudinal enhancement of the hyperechoic regions in ultrasonography of muscles using a Gabor filter bank approach: A preparation for semi-automatic muscle fiber orientation estimation," *Ultrasound Med. Biol.*, vol. 37, no. 4, pp. 665–673, 2011.
[12] M. Rana, G. Hamarneh, and J. M. Wakeling, "Automated tracking of muscle fascicle orientation in B-mode ultrasound images," *J. Biomech.*, vol. 42, no. 13, pp. 2068–2073, 2009.
[13] I. D. Loram, C. Maganaris, and M. Lakie, "Use of ultrasound to make noninvasive *in vivo* measurement of continuous changes in human muscle contractile length," *J. Appl. Physiol.*, vol. 100, no. 4, pp. 1311–1323, 2006.
[14] L. Mademli and A. Arampatzis, "Behaviour of the human gastrocnemius muscle architecture during submaximal isometric fatigue," *Eur. J. Appl. Physiol.*, vol. 94, no. 5, pp. 611–617, 2005.
[15] N. J. Cronin, C. P. Carty, R. S. Barrett, and G. Lichtwark, "Automatic tracking of medial gastrocnemius fascicle length during human locomotion," *J. Appl. Physiol.*, vol. 111, no. 5, pp. 1491–1496, 2011.
[16] J. Darby, B. Li, N. Costen, I. D. Loram, and E. Hodson-Tole, "Estimating skeletal muscle fascicle curvature from B-mode ultrasound image sequences," *IEEE Trans. Biomed. Eng.*, vol. 60, no. 7, pp. 1935–1945, Jul. 2013.
[17] T. Muramatsu, T. Muraoka, Y. Kawakami, A. Shibayama, and T. Fukunaga, "*In vivo* determination of fascicle curvature in contracting human skeletal muscles," *J. Appl. Physiol.*, vol. 92, pp. 129–134, 2002.
[18] C. Maganaris, V. Baltzopoulos, and A. Sargeant, "Human calf muscle responses during repeated isometric plantarflexions," *J. Biomech.*, vol. 39, no. 7, pp. 1249–1255, 2006.
[19] J. Guo, Y.-P. Zheng, H. Xie, and X. Chen, "Continuous monitoring of electromyography (EMG), mechanomyography (MMG), sonomyography (SMG), and torque output during ramp and step isometric contractions," *Med. Eng. Phys.*, vol. 32, no. 9, pp. 1032–1042, 2010.
[20] X. Chen, Y.-P. Zheng, J.-Y. Guo, Z. Zhu, S.-C. Chan, and Z. Zhang, "Sonomyographic responses during voluntary isometric ramp contraction of the human rectus femoris muscle," *Eur. J. Appl. Physiol.*, vol. 112, no. 7, pp. 2603–2614, 2012.
[21] Y.-P. Zheng, M. Chan, J. Shi, X. Chen, and Q. Huang, "Sonomyography: Monitoring morphological changes of forearm muscles in actions with the feasibility for the control of powered prosthesis," *Med. Eng. Phys.*, vol. 28, no. 5, pp. 405–415, 2006.
[22] J. Guo, Y.-P. Zheng, Q. Huang, X. Chen, J. He, and H. L.-W. Chan, "Performances of one-dimensional sonomyography and surface electromyography in tracking guided patterns of wrist extension," *Ultrasound Med. Biol.*, vol. 35, no. 6, pp. 894–902, 2009.
[23] X. Chen, Y.-P. Zheng, J.-Y. Guo, and J. Shi, "Sonomyography (SMG) control for powered prosthetic hand: A study with normal subjects," *Ultrasound Med. Biol.*, vol. 36, no. 7, pp. 1076–1088, 2010.
[24] J. Shi, Y.-P. Zheng, Q. Huang, and X. Chen, "Continuous monitoring of sonomyography, electromyography, and torque generated by normal upper arm muscles during isometric contraction: Sonomyography assessment for arm muscles.," *IEEE Trans. Biomed. Eng.*, vol. 55, no. 3, pp. 1191–1198, Mar. 2008.
[25] H.-B. Xie, Y.-P. Zheng, J.-Y. Guo, X. Chen, and J. Shi, "Estimation of wrist angle from sonomyography using support vector machine and artificial neural network models," *Med. Eng. Phys.*, vol. 31, no. 3, pp. 384–391, 2009.
[26] J. McMeeken, I. Beith, D. Newham, P. Milligan, and D. Critchley, "The relaltionship between EMG and change in thickness of transversus abdominis," *Clin. Biomech.*, vol. 19, no. 4, pp. 337–342, 2004.
[27] M. Miyatani, H. Kanehisa, S. Kuno, T. Nishijima, and T. Fukunaga, "Validity of ultrasonograph muscle thickness measurements for estimating muscle volume of knee extensors in humans," *Eur. J. Appl. Physiol.*, vol. 86, no. 3, pp. 203–208, 2002.
[28] N. H. Raney, D. S. Teyhen, and J. D. Childs, "Observed changes in lateral abdominal muscle thickness after spinal manipulation: A case series using rehabilitative ultrasound imaging," *J. Orthopaed. Sports Phys. Ther.*, vol. 37, no. 8, pp. 472–479, 2007.
[29] K. Ohata, T. Tsuboyama, N. Ichihashi, and S. Minami, "Measurement of muscle thickness as quantitative muscle evaluation for adults with severe cerebral palsy," *Phys. Ther.*, vol. 86, no. 9, pp. 1231–1239, 2006.
[30] C. English, K. Thoirs, L. Fisher, H. McLennan, and J. Bernhardt, "Ultrasound is a reliable measure of muscle thickness in acute stroke patients, for some, but not all anatomical sites: A study of the intra-rater reliability of muscle thickness measures in acute stroke patients," *Ultrasound Med. Biol.*, vol. 38, no. 3, pp. 368–376, 2012.
[31] J. Darby, E. F. Hodson-Tole, N. Costen, and I. D. Loram, "Automated regional analysis of B-mode ultrasound images of skeletal muscle movement," *J. Appl. Physiol.*, vol. 112, no. 2, pp. 313–327, 2012.
[32] T. Koo, C. Wong, and Y.-P. Zheng, "Reliability of sonomyography for pectoralis major thickness measurement," *J. Manipulat. Physiol. Therap.*, vol. 33, no. 5, pp. 386–394, 2010.
[33] J. Shi, J.-Y. Guo, S. Hu, and Y.-P. Zheng, "Recognition of finger flexion motion from ultrasound image: A feasibility study," *Ultrasound Med. Biol.*, vol. 38, no. 10, pp. 1695–1704, 2012.
[34] C. Castellini, G. Passig, and E. Zarka, "Using ultrasound images of the forearm to predict finger positions," *IEEE Trans. Neural Syst. Rehabil. Eng.*, vol. 20, no. 6, pp. 788–797, Nov. 2012.
[35] K. Zhang, L. Zhang, and M.-H. Yang, "Real-time compressive tracking," in *Proc. 12th Eur. Conf. Comp. Vis.*, 2012, pp. 866–879.
[36] J. Seymour, K. Ward, P. Sidhu, Z. Puthucheary, J. Steier, C. Jolley, G. Rafferty, M. Polkey, and J. Moxham, "Ultrasound measurement of rectus femoris cross-sectional area and the relationship with quadriceps strength in copd," *Thorax*, vol. 64, no. 5, pp. 418–423, 2009.
[37] P. De Bruin, J. Ueki, A. Watson, and N. Pride, "Size and strength of the respiratory and quadriceps muscles in patients with chronic asthma," *Eur. Respirat. J.*, vol. 10, no. 1, pp. 59–64, 1997.
[38] Q. Huang, Y.-P. Zheng, X. Chen, J. Shi, and J. He, "Development of a frame-synchronized system for continuous acquisition and analysis of sonomyography, surface EMG and corresponding joint angle," *Open Biomed. Eng. J.*, vol. 1, pp. 77–84, 2007.
[39] G. F. Pinton, J. J. Dahl, and G. E. Trahey, "Rapid tracking of small displacements with ultrasound," *IEEE Trans. Ultrason., Ferroelectr., Freq. Control*, vol. 53, no. 6, pp. 1103–1117, Jun. 2006.
[40] H. Akima and A. Saito, "Inverse activation between the deeper vastus intermedius and superficial muscles in the quadriceps during dynamic knee extensions," *Muscle Nerve*, vol. 47, no. 5, pp. 682–690, 2013.

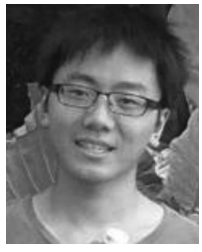

Jizhou Li was born in China, in 1989. He received the B.Sc degree in mathematics from Hunan University, China, in 2011. Since then he has been working toward the M.Sc. degree in mathematics at the College of Mathematics and Econometrics, Hunan University. He is currently a visiting student in Shenzhen Institutes of Advanced Technology, Chinese Academy of Sciences.

His current research interests include partial differential equation with applications to medical image processing, pattern recognition and machine learning.

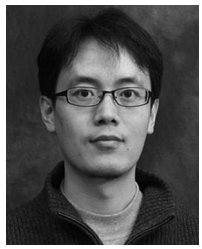

Yongjin Zhou (M'13) was born in China, in 1975. He received the B.Sc., M.Eng., and Ph.D. degrees in biomedical engineering from Xĭan Jiaotong University, Xĭan, China, in 1996, 1999, and 2003 respectively.

He is currently an Associate Professor with the Shenzhen Institutes of Advanced Technology, Chinese Academy of Sciences, Shenzhen, China. After a Postdoctoral Fellowship at the Oregon Hearing Research Center, Portland, OR, USA, he joined Hong Kong Polytechnic University (PolyU), Hong Kong, in 2005, and was there until 2012. His research interests include biological signal processing, medical ultrasound, medical image analysis, and pattern recognition.

Yi Lu was born in China, in 1989. She is currently working toward the M.S. degree in communication and information system at Wuhan University of Technology, Wuhan, China and studying as a visiting student in Shenzhen Institutes of Advanced Technology, Chinese Academy of Sciences, China.

Her research interests include signal processing and pattern recognition.

Guangquan Zhou was born in China, in 1978. He received the B.Sc. and M.S. degrees in biomedical engineering from Southeast University, Nanjing, China, in 2000 and 2003, respectively. He is working toward the Ph.D. degree from Hong Kong Polytechnic University, Hong Kong.

He was a Software Engineer for six years with the Alcatel-Lucent Technology R&D Center, Nanjing, China,. His research interests include human motion analysis, sonomyography, ultrasound imaging, and medical image processing.

Lei Wang (M'03) received the B.Eng. degree in information and control engineering and the Ph.D. degree in biomedical engineering, both from Xi'an Jiaotong University, Xi'an, China, in 1995 and 2000, respectively.

He is currently a Full Professor with the Shenzhen Institutes of Advanced Technology, Chinese Academy of Sciences, Shenzhen, China. He has published over 200 scientific papers, authored four book chapters, and filed 60 patents. His research interest includes body sensor network.

Yong-Ping Zheng (SM'06) received the B.Sc. and M.Eng. degees in electronics and information engineering from the University of Science and Technology of China, Hefei, China, and the Ph.D. degree in biomedical engineering from Hong Kong Polytechnic University (PolyU), Hong Kong, in 1997.

He is currently the Acting Head with the Interdisciplinary Division of Biomedical Engineering, PolyU. His research interests include biomedical ultrasound instrumentation, ultrasound imaging, tissue elasticity measurement and imaging, and wearable sensors for healthcare.